Membrane-Binding Peptide from the C2 Domain of Factor VIII Forms an Amphipathic Structure As Determined by NMR Spectroscopy[†,‡]

Gary E. Gilbert*[,§] and James D. Baleja[||]

Medicine Departments of the Brockton-West Roxbury VA Medical Center, Brigham and Women's Hospital, and Harvard Medical School and the Department of Biochemistry, Tufts University Medical School, Boston, Massachusetts 02111

Received November 8, 1994[⊗]

ABSTRACT: Factor VIII binds to cell membranes prior to assembling with the serine protease, factor IXa, to form the factor X-activating enzyme complex. In order to better understand the interaction between factor VIII and phosphatidylserine-containing membranes, we have synthesized the membrane-binding peptide from the C2 domain of factor VIII, corresponding to residues 2303−2324. The peptide, $fVIII_{2303-24}$, with a primary structure of TRYLRIHPQSWVHQIALRMEVL, aggregates at concentrations above 2 μM at pH 7 but is soluble at pH 6. $fVIII_{2303-24}$ competes with fluorescein-labeled factor VIII (K_i = 3 μM) for binding sites on synthetic phosphatidylserine-containing membranes and for binding sites on stimulated platelets. Circular dichroism spectra indicate that $fVIII_{2303-24}$ is predominantly a random coil in aqueous solution but adopts a predominantly helical conformation upon interaction with SDS micelles. ^{1}H NMR spectroscopy in the presence of SDS micelles allowed estimation of interproton distances from the nuclear Overhauser effect and estimation of torsion angles from coupling constants indicated by splitting of resonance lines. The distance and angle estimates, processed by distance geometry/simulated annealing software, indicate that $fVIII_{2303-24}$ has an α-helical segment encompassing residues P8−E20 and an extended segment encompassing residues L4−P8. The location of six hydrophobic residues on one face of the structure suggests that hydrophobic interactions contribute to membrane-binding. In addition, two arginines penetrate the hydrophobic plane suggesting that they interact with phosphate moieties in a phospholipid bilayer.

Factor VIII (antihemophilic factor) functions as a cofactor in the Xase enzyme complex upon the platelet membrane [for review, see Gilbert (1994)]. Within this complex, factor VIII binds both to a platelet receptor or binding site (Nesheim et al., 1988; Gilbert et al., 1991) and to the enzyme, factor IXa (Duffy et al., 1992). The assembled complex efficiently cleaves the zymogen, factor X, to factor Xa which is then responsible for catalyzing prothrombin activation (Mann et al., 1990). The importance of the assembled Xase complex is illustrated by hemophilia, a disease in which a deficiency of either factor VIII or factor IX leads to life-threatening bleeding. In spite of the critical role played by membrane binding of factor VIII, the molecular mechanisms responsible for binding to the platelet membrane are not characterized.

Factor VIII, a trace plasma protein of M_r 280 000, is homologous to another plasma protein, factor V (Church et al., 1984). The two proteins function analogously since both serve as cofactors in highly efficient enzyme complexes upon the platelet membrane (Kane & Davie, 1988; Mann et al., 1990). The proteins share a repeating domain structure of A1-A2-B-A3-C1-C2 in which the A domains are homologous with ceruloplasmin, a copper-binding plasma protein. The B domains have no homology with one another or with known proteins. The C domains share homology with discoidin, a phosphatidylserine-binding lectin (Bartles et al., 1982), and with murine milk fat globule membrane protein (Stubbs et al., 1990). Both proteins form heterodimers with an A1-A2 "heavy chain" and an A3-C1-C2 "light chain". The light chains of both proteins bind to activated platelets (Nesheim et al., 1988; Sims et al., 1988) and to phosphatidylserine-containing membranes (van de Waart et al., 1983; Pusey & Nelsestuen, 1984; Gilbert et al., 1991) while the heavy chains do not. Current data suggest that an amino acid sequence(s) responsible for membrane binding of factor VIII can be further localized to the carboxyl-terminal region of the C2 domain. A monoclonal antibody, NMC-VIII/5, that recognizes an epitope corresponding to amino acids 2170−2327 and a human alloantibody called TK that recognizes an epitope corresponding to residues 2248−2312 within the terminal portion of the C2 domain block binding of factor VIII to phosphatidylserine in microtiter wells (Shima et al., 1993). In addition, synthetic peptides corresponding to this epitope block binding of factor VIII to phosphatidylserine in the same assay (Foster et al., 1990). Like factor VIII, factor V has a membrane-binding function in the C2 domain (Ortel et al., 1992; Kalafatis et al., 1994).

To better understand the membrane-binding mechanism, we investigated whether a synthetic peptide corresponding to the phosphatidylserine-binding region of the factor VIII C2 domain would compete for factor VIII binding sites on

[†] This work was supported by the Medical Research Service of the Department of Veterans Affairs, Tufts University, and NIH Grant No. HL42443. G.E.G. is the recipient of NIH Clinical Investigator Award No. HL02587.

[‡] This information has been deposited in the Protein Data Bank, Brookhaven National Laboratories (file name 1CFG) and is also available, together with coordinates for all calculated structures from the authors via electronic mail (jbaleja@opal.tufts.edu).

* Address correspondence to this author at Brockton-West Roxbury VA Medical Center, 1400 VFW Parkway, West Roxbury, MA 02132. Phone: (617) 323-3427. Fax: (617) 323-8786.

[§] Brockton-West Roxbury VA Medical Center, Brigham and Women's Hospital, and Harvard Medical School.

[||] Tufts University Medical School.

[⊗] Abstract published in *Advance ACS Abstracts,* January 1, 1995.

0006-2960/95/0434-3022$09.00/0 © 1995 American Chemical Society

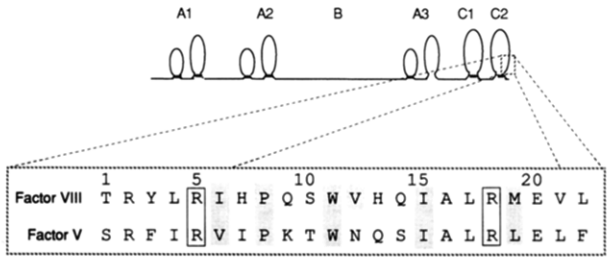

FIGURE 1: Membrane-binding peptide from the C2 domain of factor VIII, $fVIII_{2303-24}$. The domain structure of factor VIII is illustrated by the line figure above. Disulfide bonds are illustrated by short lines closing loops, based upon the assumption that factor VIII cysteine pairs, homologous to those of factor V, oxidize to form homologous bonds (Xue et al., 1993a,b). The inset depicts the amino acid sequence of the membrane-binding peptide from factor VIII and the corresponding sequence from factor V. The factor VIII amino acids with gray borders are hydrophobic residues that reside on the hydrophobic surface when the peptide is folded into its membrane-binding conformation (see Figures 10 and 11), and the black borders indicate arginines that reside on the hydrophobic surface at either end of the α-helix. The corresponding hydrophobic and Arg residues of factor V are also indicated by gray and black borders, respectively.

defined membranes and on platelet membranes. Upon confirming that a 22 amino acid peptide has these properties, we determined the three-dimensional structure using NMR[1] spectroscopy. We studied the peptide bound to micelles of perdeuterated SDS because these small micelles provide a membrane-like environment in which narrow NMR resonances are obtainable (Macquaire et al., 1993; McDonnell & Opella, 1993; Plesniak et al., 1993; Popot, 1993; Reynaud et al., 1993; Wang et al., 1993; Franklin et al., 1994). The results show that the peptide forms an amphipathic structure with an extended amino-terminal region and an α-helix in the carboxyl-terminal region. This structure has features that both resemble and differ from those of other membrane-binding peptides.

MATERIALS AND METHODS

Bovine brain phosphatidylserine and egg yolk phosphatidylcholine were from Avanti Polar Lipids, Pelham, AL. Cholesterol was from Calbiochem. Fluorescein-5-maleimide was from Molecular Probes, Eugene, OR.

The peptide, $fVIII_{2303-24}$ (Figure 1) was synthesized using an Applied Biosystems Inc. 430A peptide synthesizer with the 9-fluorenylmethoxycarbonyl method. The product was purified by collecting the single dominant elution peak from high performance liquid chromatography on a C18 column (Beckman). The amino acid sequence was confirmed by sequencing on an Applied Biosystems Inc. 470A protein sequencer.

Recombinant human factor VIII, a generous gift from Debbie Pittman (Genetics Institute, Cambridge, MA), was labeled with fluorescein maleimide as described (Gilbert et al., 1991, 1992). Lipid bilayers supported by glass microspheres (lipospheres) were prepared by allowing sonicated phospholipid vesicles (Barenholz et al., 1977) to fuse on clean glass microspheres of 2.0 μm diameter (Gilbert et al., 1992). Lipospheres were stored at 4 °C in the dark and used within 30 h of preparation. Binding of fluorescein-labeled factor VIII to lipospheres was evaluated by flow cytometry using a Coulter Epics Profile II (Gilbert et al., 1992).

Gel filtered platelets were prepared as previously described (Gilbert et al., 1991). Platelets were stimulated by 2 μM A23187, diluted into a suspension of platelets at 1×10^8/mL from a 200 μM stock solution in dimethyl sulfoxide. Binding of factor VIII to stimulated platelet was measured by flow cytometry as described for lipospheres (Gilbert et al., 1992).

For circular dichroism studies, lyophilized peptide was dissolved in 50 mM NaCl, 5 mM Na_2HPO_4, and 5 mM NaH_2PO_4, pH 5.5 and held in a 0.4 cm path length cuvette at 35 °C. Spectral data were obtained at 0.5 nm increments, 1.5 nm bandwidth, with an AVIV Model 60 DS spectropolarimeter. Displayed spectra represent the simple average of three spectra smoothed once with the smoothing algorithm supplied in the AVIV software.

For NMR studies lyophilized peptide (2.3 mM) was solubilized in a buffer containing 80 mM SDS-d_{25} (Cambridge Isotopes, Woburn, MA), 50 mM NaCl, 5 mM Na_2HPO_4, and 5 mM NaH_2PO_4, pH 5.5. Samples in H_2O also contained 10% D_2O for the deuterium lock signal. Spectra were collected, mostly at 35 °C, on a Bruker AMX-500 spectrometer with a proton frequency of 500.14 MHz. The carrier frequency was set on the water resonance, which was suppressed using presaturation. Two-dimensional NOESY spectra were acquired with mixing times of 75 and 150 ms, 96 summed scans, 2048 real t_2 points with a spectral width of 8065 Hz, 512 t_1 TPPI increments, and a relaxation delay of 1.3 s between scans. Spectra were apodized with a sine bell shifted by 45° in t_2 (applied over 1024 points) and with a squared sine bell shifted by 60° in t_1 (applied over all 512 points). The matrix was zero-filled to a 2K by 1K (real) points, and baselines of the 2D spectra were flattened using the Bruker NMR processing program. NOESY cross-peak intensities were measured using the Bruker 2D integration routine. They were converted into distances using the intensities corresponding to the 2.5 Å separations between neighboring protons of the well-ordered tryptophan side chain as a reference and a distance extrapolation procedure (Baleja et al., 1990). A TOCSY spectrum was collected and processed using identical parameters as the NOESY, except with a mixing time of 44 ms using an MLEV-17 mixing sequence and 64 summed scans (Bax & Davis, 1985). A DQF-COSY spectrum was collected with 2048 real t_2 points with a spectral width of 8065 Hz, 768 t_1 TPPI increments, and a relaxation delay of 1.3 s between scans. Spectra were apodized with sine bells shifted by 30° in t_2 and 45° in t_1 and zero-filled to a 2K by 1K (real) matrix.

Protons were assigned to their resonance positions following standard homonuclear methods. These consist of establishing intraresidue connectivities via the TOCSY and DQF-COSY experiments followed by a search for sequential $d_{\alpha N}$, d_{NN}, and $d_{\beta N}$ cross-peaks in the NOESY spectrum (Wüthrich, 1986).

1D spectra were collected in D_2O solution between 20 and 45 °C to confirm stability of the peptide over this temperature range and to clearly observe some particular α proton resonances, which, at a given temperature, are under the water resonance. A NOESY spectrum was collected in D_2O solution at 25 °C using 1.1 mM peptide concentration, 64

[1] Abbreviations: SDS, sodium dodecyl sulfate; NMR, nuclear magnetic resonance; TOCSY, total correlation spectroscopy; DQF-COSY, double-quantum-filtered correlation spectroscopy; TPPI; time-proportional phase incrementation; NOE, nuclear Overhauser effect; NOESY, NOE spectroscopy; DG/SA, distance geometry/simulated annealing; RMS, root-mean-square.

scans, a 50 ms mixing time, and a spectral width of 5000 Hz.

Experimentally, torsion angles are inferred from the coupling constants measured using cross-sections of NOE cross-peaks along ω_2 in spectra resolution-enhanced by processing with 20° shifted sine bells applied over 2048 (real) points in t_2, effectively resulting in line widths of 4−5 Hz. Some amide protons exhibited coupling constants greater than 6 Hz—the remainder had splittings of less than 6 Hz. ϕ dihedral angles were constrained to the negative ϕ angle region from consideration of the HN−Hα coupling constants and the NOE intensities for intraresidue αN and the sequential NN and α,N(i+1) NOE cross-peaks. For samples in D_2O solution, coupling constants to the β proton were measured for isoleucine, threonine, and valine residues. For some of the other residues, NOE cross-peaks between the α proton and amide proton to the β protons allowed stereospecific proton assignment and characterization of the χ_1 torsion angle.

Initial structure generation used a set of approximately 300 interproton distance restraints and a set of 27 torsion angle measurements. Ten structures were generated using distance geometry/simulated annealing (DG/SA) methods (Havel, 1991) and examined using InsightII (Biosym Technologies, San Diego, CA). The initial structures had a backbone RMS deviations of less than 1 Å. Several close (<3 Å) approaches of protons were noted which were absent from the NOESY spectra. In addition, several NOEs, which were previously ambiguous from reliance on chemical shift data alone, were now clearly assignable to unique proton pairs. Finally, error violations of greater than 0.2 Å were compiled from the structures. Most errors were the results of incorrect integration of cross-peaks due to spectral overlap or baseline distortions. Where it was not possible to deconvolute the peaks or correct for spectral overlap, the upper and lower limits were expanded to reflect the uncertainty in the distance restraint. After two rounds of initial structure generation, a final computation used a set of 458 interproton distances and the 27 torsion angles to generate 20 structures, all of which converged. Average torsion angles were obtained from the values of the 20 structures following a vector addition methodology (Hyberts et al., 1992). Using the backbone atoms of the well-defined residues (i.e., standard deviations of ϕ and ψ torsion angles of less than 20°), the structures were superimposed to the DG/SA structure with the lowest energy violations.

RESULTS

We have synthesized and purified a 22 amino acid peptide corresponding to the carboxyl-terminal portion of the factor VIII C2 domain ($fVIII_{2303-24}$) (Figure 1). Our selection of this peptide was influenced by the capacity of peptides containing this sequence to compete with factor VIII for binding to immobilized phosphatidylserine (Foster et al., 1990) and by the capacity of a monoclonal antibody NMC-VIII/5, with an epitope including this sequence, to block binding of factor VIII to immobilized phosphatidylserine and to phosphatidylserine-containing membranes. Furthermore, we have found that the monoclonal antibody ESH8, with an epitope corresponding to residues 2248−2307, does not efficiently block binding of factor VIII to phosphatidylserine-containing membranes.[2] Thus, these data suggest that the 2307−2327 region is critical for the phosphatidylserine-binding function. The peptide that we synthesized has nine amino acid residues that are identical to the corresponding peptide of factor V including the proline at position 8. Other features of $fVIII_{2303-24}$, shared in common with factor V, include a positive net charge related to the presence of three Arg residues and two His residues and scattered hydrophobic residues.

In preliminary experiments we observed that $fVIII_{2303-24}$ inhibited binding of factor VIII to phospholipid vesicles at pH 7.5 (not shown). However, at a concentration of 1−3 μM the peptide aggregated, precluding quantitative studies. We then observed that the peptide was soluble at pH 6, likely due to the protonated state of the two histidines at the lower pH. We next investigated the effect of low pH upon binding of factor VIII to phospholipid membranes supported by glass microspheres. Fluorescein-labeled factor VIII bound saturably to lipospheres with membranes of 15% phosphatidylserine and the quantity of factor VIII bound and the affinity were equivalent over a pH range of 7.5−6.0 (not shown). However, at pH 5.5 the quantity of bound factor VIII was decreased, and therefore the membrane binding studies were performed at pH 6.0.

$FVIII_{2303-24}$ competed with fluorescein-labeled factor VIII for binding sites on lipospheres (Figure 2A). The K_i was 3 μM indicating that this peptide binds to membrane sites with moderately high affinity. To determine whether $fVIII_{2303-24}$ also binds to the factor VIII binding sites on stimulated platelets, we performed competition binding studies with gel-filtered platelets (figure 2B). After platelets were stimulated with the calcium ionophore A23187, they were diluted into a mixture of $fVIII_{2303-24}$ and fluorescein-labeled factor VIII at pH 6.0. $FVIII_{2303-24}$ competed with factor VIII, and again the K_i was 3 μM. These data suggest that $fVIII_{2303-24}$ binds to the factor VIII binding sites on both synthetic phosphatidylserine-containing membranes and stimulated platelets.

We employed circular dichroism to determine whether $fVIII_{2303-24}$ exhibits a stable membrane-binding conformation in an aqueous solution or whether the membrane-binding conformation must be induced (Figure 3). In a phosphate buffer the spectrum of $fVIII_{2303-24}$ was characterized by a minimum at approximately 200 nm and a shape implying a small portion of β sheet or α helical conformation but predominantly a random coil conformation. After addition of 5 mM SDS the spectrum changed substantially with new minima at 208 and 224 nm. This degree of change implied an extensive conformational change, and the new minima are consistent with a conformation that is predominantly helical. Addition of SDS to higher concentrations (20 and 80 mM) did not further affect the spectra, indicating that virtually all of the peptide was bound to micelles at the 5 mM SDS concentration.

We wished to define the detailed three-dimensional structure of $fVIII_{2303-24}$ that is responsible for membrane binding; therefore, we examined its ^1H NMR spectrum. In aqueous solution at pH 5.8, 25 °C resonance lines were sharp, amide proton exchange was rapid, and chemical shifts of amide protons were characteristic of a random coil indicating a largely unstructured conformation. These data are consistent with the circular dichroism spectrum obtained under

[2] D. Scandella, G. E. Gilbert, M. Shima, C. Eagleson, M. Felch, R. Prescott, K. J. Rajalakshimi, and E. Saenko, manuscript submitted.

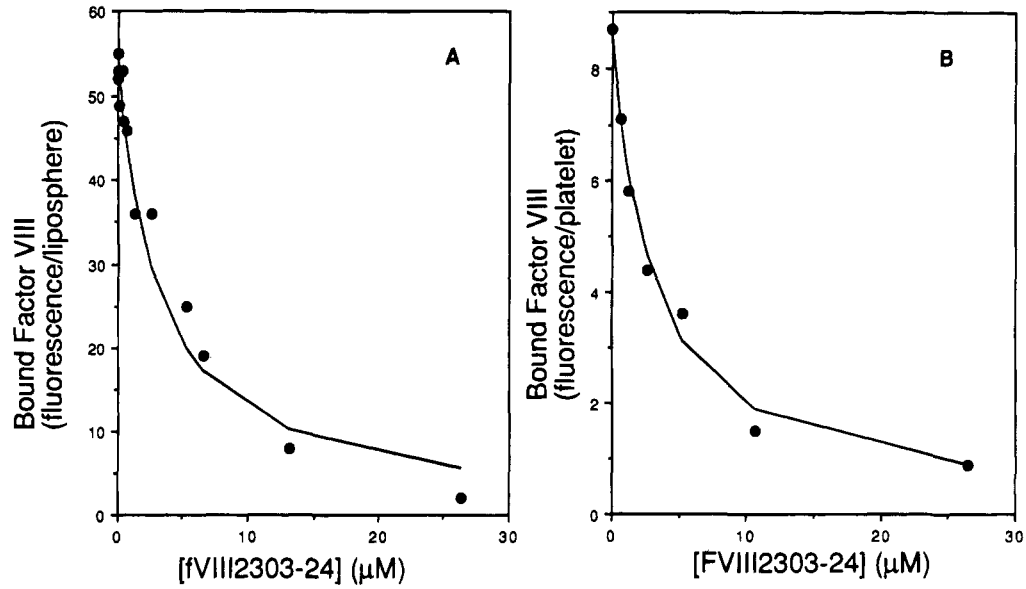

FIGURE 2: Competition between $fVIII_{2303-24}$ and factor VIII for membrane binding sites. Lipospheres (A) or platelets (B) were added to various concentrations of $fVIII_{2303-24}$ and 4 nM fluorescein-labeled factor VIII. After 10 min the quantity of bound factor VIII was measured by flow cytometry. $FVIII_{2303-24}$ competed for factor VIII binding sites on lipospheres (A) and on stimulated platelets(B). The lines indicate the calculated factor VIII bound if $fVIII_{2303-24}$ competes for factor VIII binding sites with a K_d of 3 μM. The buffer was 0.14 M NaCl, 0.02 M MES, 0.5 mM $CaCl_2$, 0.004% Tween 80, and 0.1% BSA, pH 6.0. The liposphere membrane composition was phosphatidylserine/phosphatidylcholine/cholesterol, 15:85:20.

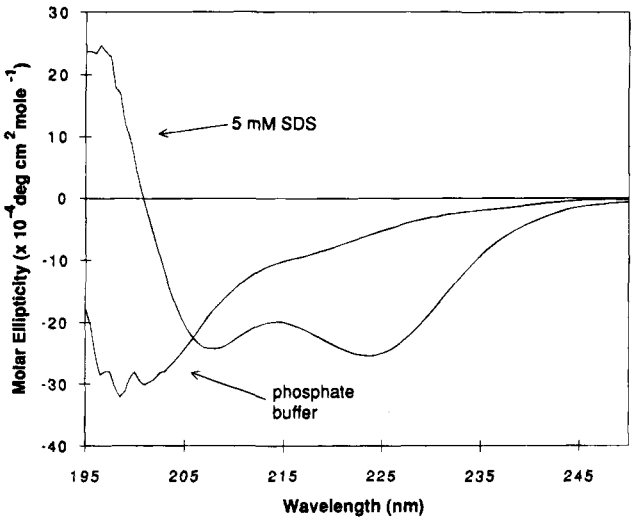

FIGURE 3: Circular dichroism spectra of $fVIII_{2303-24}$ in an aqueous solution and in detergent micelles. In an aqueous solution the CD spectrum has a minimum at approximately 200 nm consistent with a predominantly random coil conformation. After addition of SDS the spectrum has minima at 208 and 224 nm, consistent with a predominantly helical structure. The peptide is at 24 μM in 50 mM NaCl buffered by 10 mM sodium phosphate at pH 5.5, 35 °C, with and without 5 mM SDS.

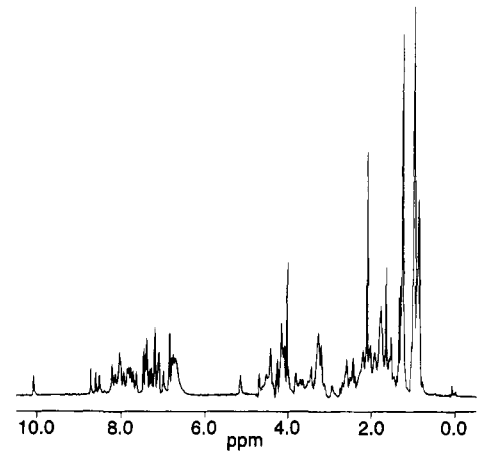

FIGURE 4: ^1H NMR spectrum of $fVIII_{2303-24}$. The spectrum for $fVIII_{2303-24}$ shows dispersion of resonances, which indicates an ordered structure in the presence of SDS micelles. The peptide is solubilized in SDS-d_{25} at pH 5.5, 35 °C.

similar conditions (Figure 3). On addition of a stoichiometric amount of deuterated SDS, the NMR spectrum disappeared, which we attributed to aggregation of the peptide upon binding of detergent monomers as previously described (O'Neil & Sykes, 1989). Upon further addition of SDS (to 80 mM), now in excess of the peptide concentration and the critical micelle concentration, the NMR spectrum was restored (Figure 4). Under these conditions, the resonance lines are disperse, indicating an ordered structure. For example, an α proton from a residue (identified as His 7) is at 5.1 ppm, downfield of the water resonance. In unstructured peptides, this proton appears near 4.6 ppm (Wüthrich, 1986). Likewise, the amide protons do not appear together as a single broad resonance of overlapping peaks near 8.4 ppm, but are spread out uniformly between 7.5 and 8.5 ppm. This indicates that the amide protons are in unique chemical environments caused by the folding of the peptide.

Two-dimensional NMR spectra were then recorded to assign protons to their resonance positions and to gather sufficient conformational data with which to define the three-dimensional structure. By a combination of NOESY and TOCSY data and by using standard homonuclear methods (Wüthrich, 1986), chemical shifts were determined for all protons in the peptide (Table 1). The chemical shifts are not unusual, except for the α proton and one of the δ protons of P8 and the γ protons of both I6 and I15, which are shifted more than 0.3 ppm away from random chemical shift values (Wishart et al., 1991). This suggests that these protons were in close proximity to the aromatic amino acid side chain of either W11 or Y3 (see below). In addition, most of the amide chemical shifts were upfield of 8.3 ppm, consistent with an α helical structure for the peptide. Modest modification of experimental conditions, i.e., 1 mM peptide and 23 mM SDS, pH 6.3, did not alter chemical shifts or cross-peak intensities.

Table 1: ^{1}H Chemical Shift Assignments for Factor VIII$_{2303-24}$ Peptide in SDS Micelles[a]

residue	NH	α	β	γ	others
Thr 1		3.98	4.18	1.25	
Arg 2	8.47	4.38	1.75	1.54	Hδ, 3.18; Hε, 7.07
Tyr 3	8.12	4.64	2.92, 3.13		Hδ, 7.18; Hε, 6.83
Leu 4	7.92	4.47	1.76	1.65	Mδ, 0.95, 1.02
Arg 5	8.20	4.32	1.88, 1.95	1.70	Hδ, 3.27; Hε, 7.10
Ile 6	7.17	4.34	1.90	*1.20, 1.40*	Mγ, 0.98; Mδ, 0.88
His 7	7.98	5.12	3.18, 3.29		Hδ, 7.37; Hε, 8.58
Pro 8		3.62	*1.78, 1.88*	*1.90, 1.63*	Hδ, *3.80, 3.42*
Gln 9	8.50	4.02	2.02, 2.10	2.41	Hδ, 6.73, 7.35
Ser 10	8.03	4.39	4.05, 4.07		
Trp 11	7.77	4.67	*3.48, 3.31*		Hδ1, 7.29; Hε3, 7.44; Hζ2, 7.43; Hζ3, 6.98; Hη2, 7.08; Hε1, 10.05
Val 12	7.82	3.68	2.17	0.87, 0.97	
His 13	8.04	4.48	3.41		Hδ, 7.39; Hε, 8.70
Gln 14	7.98	4.12	2.27, 2.30	2.57	Hδ, 6.77, 7.37
Ile 15	8.02	3.78	2.02	1.18, 1.78	Mγ, 0.94; Mδ, 0.86
Ala 16	8.19	4.07	1.49		
Leu 17	7.67	4.10	1.78, 1.63	1.53	Mδ, 0.84, 0.84
Arg 18	7.74	4.22	2.02, 2.05	1.78	Hδ, 3.25, Hε, 7.25
Met 19	7.84	4.48	*2.23, 2.10*	*2.62, 2.65*	Mε, 2.03
Glu 20	7.80	4.38	2.11, 2.20	2.48, 2.55	
Val 21	7.62	4.14	2.18	0.97, 0.97	
Leu 22	8.48	4.66			

[a] Assignments are in ppm, relative to 2,2-dimethyl-2-silapentane-5-sulfonate. Chemical shifts were assigned at pH 5.5, 35 °C, in 80 mM SDS-d_{25}, 50 mM NaCl, 5 mM Na_2HPO_4, and 5 mM NaH_2PO_4, pH 5.5. Protons assigned stereospecifically are listed in italics, with the H^2 given first and the H^3 second.

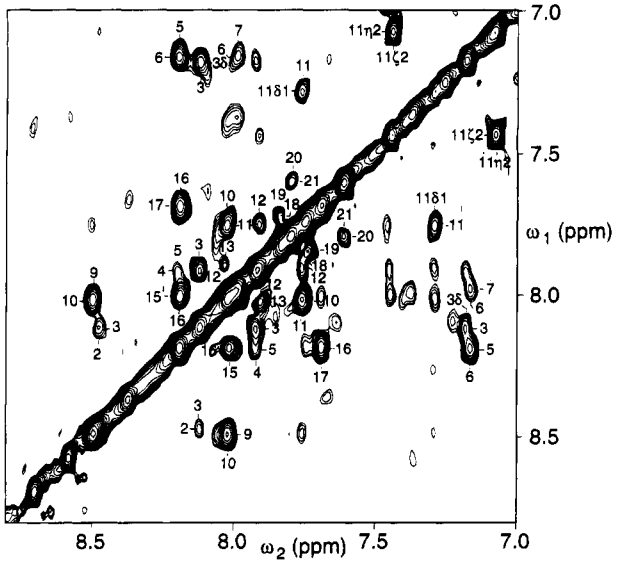

FIGURE 5: NH−NH region of the NOESY spectrum illustrating the α-helical character of the peptide. The NOE mixing time is 150 ms. Cross-peaks involving sequential amide protons are identified by residue numbers. Cross-peaks to aromatic side chain resonances in this region are indicated by the residue number and proton position (e.g., 11δ1). Experimental conditions are the same as those for Figure 4.

This confirmed that the peptide concentration, the SDS/peptide ratio, and the pH were not critical under the conditions employed.

In the NOESY spectrum (Figure 5) cross-peaks occur between amide protons of most sequential residue pairs, with strong cross-peaks for from residue 9 through 20 (Figure 6). These strong interactions and NOEs between the α proton of residue i and the β and amide proton of residue i+3, and others, suggested an α helical structure for the C-terminal portion of the peptide, with a few residues (Y3−I6) in a turn of α helix near the N-terminus, and the intervening residues (H7 and P8) in an extended conformation. The coupling constant data were also consistent with an α helical structure between residues 9 and 20, with ^3J(NH,α) below 6 Hz for all of these residues. Only residues I6 and H7 had large ^3J(NH,α), indicating the ϕ torsion angle of an extended structure.

Numerous NOE cross-peaks among side chain protons, especially between the tryptophan ring and nearby moieties, indicated well-ordered side chains. For example, NOEs were observed between the ε3 proton of Trp 11 and the α proton of Pro 8, between Trp 11ε3 and Val 12α, between Trp 11ζ2 and the β1 proton of Pro 8, between Trp 11 δ1 and Pro 8α, and between Trp 11η2 and γ and δ methyl groups of Ile 6 (Figure 7). Other NOEs to the tryptophan ring and additional NOEs, such as the γ methyl of Ile 15 to the γ protons of Met 19, are given in the supplementary material. These NOE cross-peaks between neighboring hydrophobic side chains were indicative of a well-ordered hydrophobic region on one face of the peptide. Some side chain conformations outside this patch on the opposing face were constrained by other NOEs. For example, the isolated peak at the upper left corner of Figure 7 represents a medium-strength NOE between the ε proton of His 13 and the methyl group(s) of Leu 17. The orientations of the His 7 and His 13 side chains were constrained by NOEs to peptide backbone. Throughout the helical portion of the molecule side chain orientations were constrained by observed NOEs between the α protons and the β protons of the i+3 residues (Figure 6 and supplementary material). The exact side chain conformations for residues Arg 5, Gln 9, Ser 10, Gln 14, and Arg 18 were difficult to determine because of overlapping, or nearly overlapping, β protons. Although a defined conformation was not determined for these residues, the data do not suggest that they are intrinsically mobile. Unlike the terminal residues (Thr 1, Arg 2, Tyr 3, Leu 4, Val 21, and Leu 22) their NH−α and α−β cross-peaks in NOESY spectra collected using a short mixing times did not show any antiphase cross-peaks resulting from zero quantum coherences (data not shown) (Ernst et al., 1987).

NOESY intensities were converted into interproton distances and coupling constants into torsion angles (see Materials and Methods). Distance geometry and simulated annealing were used to generate three-dimensional models consistent with the NMR data consisting of 458 interproton distances and 27 torsion angle constraints. Twenty separate calculations resulted in structures with no large violations of the restraints and with good stereochemistry. The largest violation for any distance restraint is 0.3 Å. As a guide for superimposition of the structures, average torsion angles were first obtained from the values of all 20 structures following a vector addition methodology (Hyberts et al., 1992). The average ϕ, ψ, and χ_1 torsion angles are shown in Figure 8. The backbone torsion angles (ϕ and ψ) are well determined for residues 4−19. Residues L4, R5, and residues P8−E20 have torsion angles of α-helical character ($\phi = -57 \pm 30°$, $\psi = 0$ to $-180°$). Within this region, only the hydrophobic amino acids have well defined side chains, consistent with the large number of NOEs to the side chains of these residues.

The calculated structures for the membrane-binding factor VIII peptide were superimposed over residues 4−19 since these residues have uniformly well defined ϕ and ψ torsion angles (Figure 9). The pair-wise RMS deviation for super-

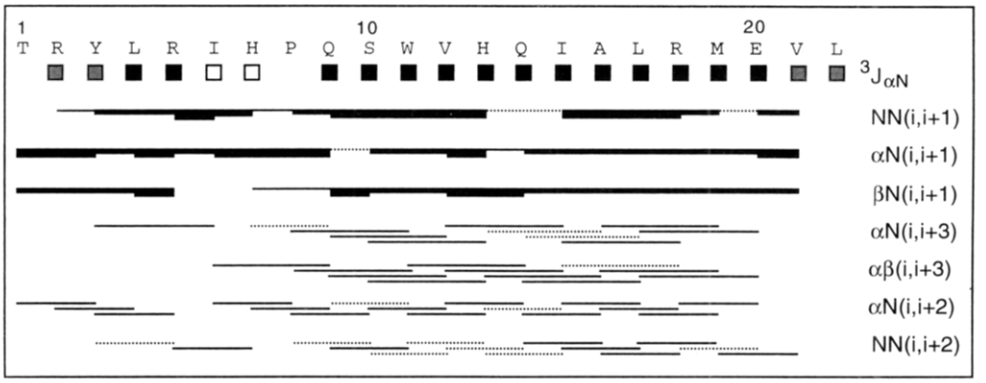

FIGURE 6: Summary of sequential and medium-range NOEs. The sequence is given with one-letter symbols of the amino acids and renumbering the sequence of the factor VIII peptide with residue 2303 designated as residue 1. The first three lines below the sequence give (i,i+1) connectivities, which were analyzed quantitatively from a 75 ms NOESY spectrum. Since the δ protons of proline occupy a position approximately equivalent to the amide proton of other residues, for P8, NOEs to the proline δ protons are reported as amide ("N") entries. A thin line indicates a weak NOE, and a thick line, a strong one. Medium-range NOEs typical for helical structures are listed in the lower four lines. Clearly missing NOE cross-peaks are indicated by a blank space. Other NOE cross-peaks, possibly obscured by resonance overlap, are indicated with a dotted line. Coupling constants to amide protons are indicated at the top of the figure. Black boxes are used for $^3J_{NH.\alpha} < 6$ Hz, open boxes for $^3J_{NH.\alpha} \geq 8$ Hz, and shaded boxes for $^3J_{NH.\alpha}$ between 6 and 8 Hz.

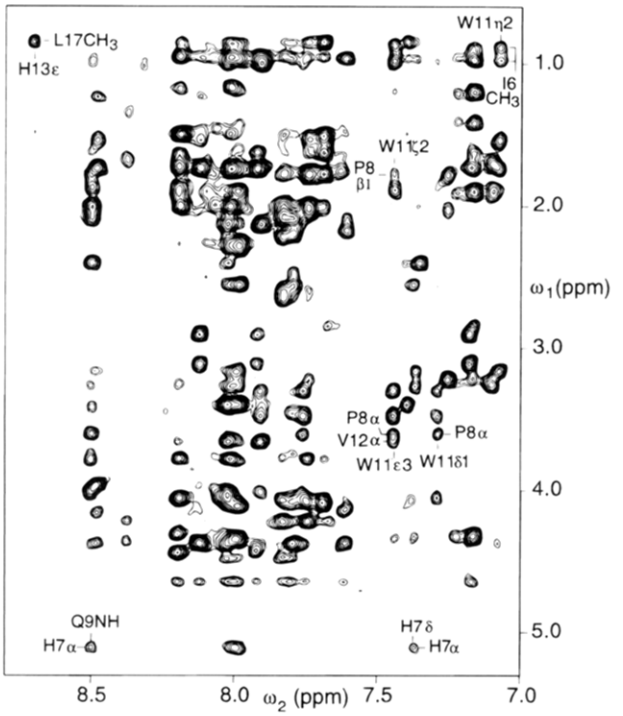

FIGURE 7: Two-dimensional NOESY spectrum illustrating cross-peaks that include side chain protons. An NOE was observed between the ϵ proton of H13 and the methyl protons of L17 (upper left corner) locating these side chain protons within a few angstoms of each other. A cross-peak between the α proton of H7 and the amide proton of Q9 (lower left corner) indicates that these residues are adjacent to each other, as predicted by the backbone conformational data. A series of NOE cross-peaks between protons of W11 and those of P8, V12, and I6 (right midsection to upper corner) indicate that the corresponding hydrophobic side chains are clustered close together at the beginning of the helical region. Cross-peaks between W11 and I6 are clearly resolved from those between W11 and I15 in the complementary region of the spectrum on the opposite side of the diagonal (not shown). These peaks indicate that the I15 side chain is located close to W11 with the other hydrophobic residues.

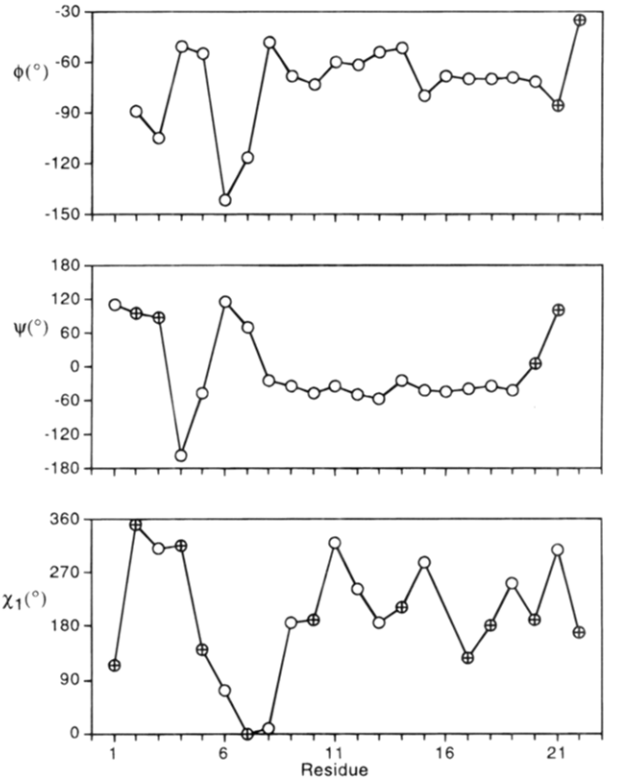

FIGURE 8: Average torsion angles ϕ, ψ, and χ_1 for the fVIII$_{2303-24}$. Twenty structures were calculated for the peptide using DG/SA with sets of interproton distances and torsion angles as restraints (see text). As a guide to superimpose the structures, average torsion angles were first obtained from the values of all 20 structures following a vector addition methodology (Hyberts et al., 1992). Angles shown with open circles have standard deviations of less than 20°, and angles shown with crossed circles are less well defined. The backbone torsion angles (ϕ and ψ) are well determined for residues 4−19. Within this region, only hydrophobic amino acids have well defined side chains. Residues with torsion angles of α-helical character ($\phi = -57$, $\psi = -47$) include residues L4, R5, and P8−E20.

imposed atoms is 0.6 ± 0.2 Å. The pair-wise RMS deviation for all atoms in this region is 1.6 ± 0.3 Å. Features of the structure include three or four unstructured N-terminal amino acids, two or one residues with α-helical torsion angles, two residues in an extended conformation, and a long, well-defined α helix beginning at *trans* proline 8 and ending with methionine-19. The C-terminal two or three residues are unstructured. The amide protons of I15−R18 participate in hydrogen bonds typical of α helices (with carbonyl of residue i−4 acting as the hydrogen bond acceptor). In addition, there is a hydrogen bond between the amide of S10 and the carbonyl of H7, and, in the majority of the calculated

FIGURE 9: Stereoview overlay of 20 calculated structures for the membrane-binding factor VIII peptide. Residues 4−19 have uniformly well defined ϕ and ψ torsion angles. Therefore, using the backbone atoms of these residues, the structures were superimposed to the DG/SA structure with the lowest energy violations. The pair-wise RMS deviation for superimposed atoms is 0.6 ± 0.2 Å. A well-defined α helix extends from P8 to M19.

structures, hydrogen bonds are observed between the amides of M19, E20, and V21 and the carbonyls of A16, A16, and M19, respectively.

Display of the amino acid side chains attached to the backbone within the well-ordered region of the peptide demonstrates that the hydrophobic residues reside along one face of the helix (Figure 10). Arg 5 extends into the hydrophobic plane at one end of the helix, and Arg 18 penetrates the plane at the other end. The unusual chemical shifts noted above can be satisfactorily explained by the ring current shifts of the tryptophan side chain—protons of the proline side chain are shifted upfield since they are located near, above, and perpendicular to the tryptophan ring plane, whereas the protons of the I6 and I15 side chains are shifted downfield since they are within the tryptophan ring plane (Wüthrich, 1986).

The amphipathic nature of the membrane-binding peptide from factor VIII is revealed clearly by viewing the structure with the long axis of the helix perpendicular to the page (Figure 11). Most of the hydrophobic groups are localized to one face of the structure. These data suggest the $fVIII_{2303-2324}$ aligns with a micelle or a membrane in such a way that the hydrophobic face is in contact with the hydrophobic phospholipid or detergent acyl chains.

DISCUSSION

Our studies indicate that a 22 amino acid peptide from the C2 domain of factor VIII ($fVIII_{2303-24}$) binds to phosphatidylserine-containing membranes and to activated platelets, thereby competing for factor VIII binding sites. These results, in combination with the prior demonstration that a peptide containing the same sequence competes with factor VIII for binding to pure phosphatidylserine (Foster et al., 1990), suggest that the stereoselective phosphatidylserine-binding motif of factor VIII (Gilbert & Drinkwater, 1993) is located within $fVIII_{2303-24}$. Although $fVIII_{2303-24}$ is a constituent of a large protein, it blocks the highly specific membrane binding sites (Gilbert et al., 1992; Gilbert & Drinkwater, 1993) recognized by factor VIII (Figure 2) independent of the remainder of the protein and is, in turn, recognized by anti-factor VIII antibodies that block the membrane binding function of factor VIII.[2] These properties suggest that this 22 amino acid peptide can assume the native membrane-binding structure. As a first step toward understanding the membrane-binding properties, we have solved the three-dimensional structure of the peptide using two-dimensional ^1H NMR. Like other membrane-binding peptides, $fVIII_{2303-24}$ responded to the membrane-like environment of SDS micelles by assuming a stable structure. Features of the structure include an extended amino-terminal 8 amino acid section and a 12 amino acid α-helix in which the hydrophobic amino acids are exposed on one face. This structure suggests that $fVIII_{2303-24}$ binds to membranes in a configuration where the hydrophobic amino acid residues penetrate the hydrophobic core of the membrane.

Platelets develop procoagulant activity in parallel with the reorientation of phosphatidylserine from the inner to the outer bilayer of the plasma membrane (Bevers et al., 1983). Under the same conditions that lead to phosphatidylserine reorientation, platelets express specific receptors/binding sites for

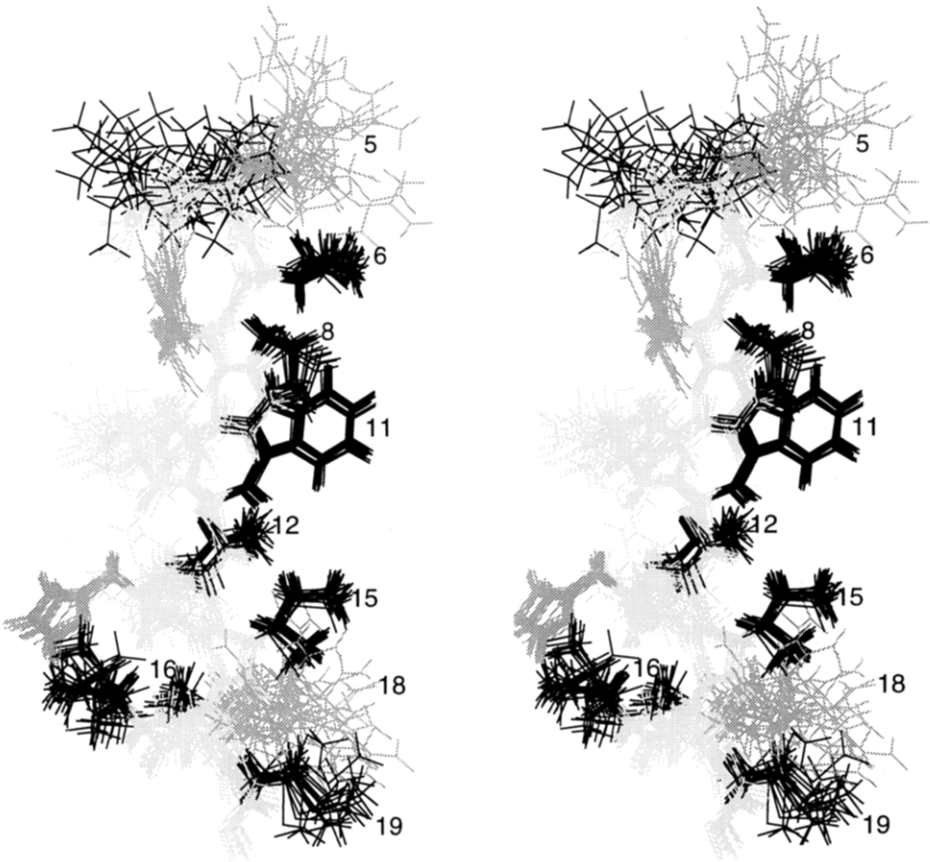

FIGURE 10: Structures for the well-defined portion of the membrane-binding factor VIII peptide. Structures are shown for the well-defined residues 4−19 including the side chains. The pair-wise RMS deviation for all atoms in this region is 1.6 ± 0.3 Å. Hydrophobic amino acid side chains (L4, I6, P8, W11, V12, I15, A16, L17, and M19) are shown in bold, positively charged amino acids (R5, H7, H13, and R18) are shown in dark gray, and the rest of the molecule is shown in light gray. The labeled residues form a well defined hydrophobic patch flanked by two loosely defined arginines on the right side of the molecule. L4 is visible in the top left part of the molecule. It is, however, ill-defined.

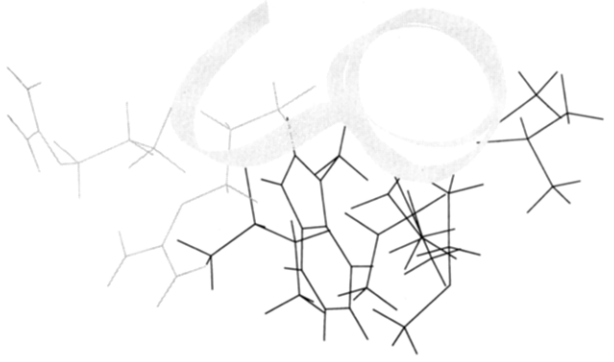

FIGURE 11: Amphipathic nature of the membrane-binding peptide from factor VIII is revealed best by viewing the α helix end-on. The DG/SA structure with the lowest energy violations is shown. Side chains of hydrophobic residues are shown in bold and cluster in the lower half of the model. Note that the hydrophobic patch extends beyond the α helix to include Ile 6 in the extended region of the peptide. These hydrophobic residues likely interact with the acyl chains of SDS in the interior of detergent micelles. Two arginines, shown in gray, are on the same side of the peptide as the hydrophobic patch although their conformations are not well defined (see Figure 9 for an estimate of the range of possible conformations). These cationic residues, flanking the hydrophobic patch, may interact with the negatively charged head groups of SDS.

factor VIII and support function of factor VIII in the Xase complex (Nesheim et al., 1988; Gilbert et al., 1991). When platelets are stimulated by agonists that induce procoagulant activity, they release small vesicles derived from the plasma membrane (Wolf, 1967; Sandberg et al., 1985; Sims & Wiedmer, 1986). These vesicles, also referred to as microparticles, have a high density of membrane receptors/binding sites for factor VIII (Gilbert et al., 1991). The affinity of factor VIII binding to activated platelets and to microparticles is equivalent to the affinity of binding to synthetic membranes containing phosphatidylserine. In addition, binding sites containing phosphatidylserine, like those of activated platelets, are highly specific for factor VIII (Gilbert et al., 1992). The specificity is mediated by a stereoselective interaction of factor VIII with *O*-phospho-L-serine, the head group of phosphatidylserine (Gilbert & Drinkwater, 1993). Thus, existing data support the hypothesis that phosphatidylserine-containing membrane binding sites function like receptors for factor VIII on the platelet membrane, although they do not preclude the participation of a membrane protein in the binding mechanism. These data have motivated us to study a factor VIII peptide that binds to phosphatidylserine-containing membrane binding sites.

Our data are consistent with a model in which the long axis of $fVIII_{2303-24}$ lies parallel to a membrane and the hydrophobic face interacts with the hydrophobic core of the membrane (Figure 12). We prefer this model over the alternative, in which the long axis of the helix lies perpendicular to the membrane for two reasons. First, a common structural motif of membrane binding peptides is an amphipathic helix, similar to the structure that we have solved. These structures tend to bind to membranes with the long axis of the helix parallel to the membrane plane and the hydrophobic residues interacting with membrane residues (Kaiser & Kezdy, 1983; Reynaud et al., 1993; Tytler et al.,

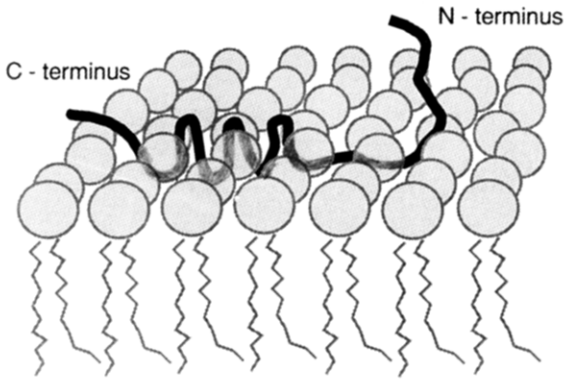

FIGURE 12: Model of $fVIII_{2303-24}$ bound to a phospholipid membrane. We hypothesize that the peptide backbone lies in the interfacial region of the bilayer with the long axis of the α-helix parallel to the membrane. This orientation permits the hydrophobic residues to penetrate the core of the membrane and interact with acyl chains. The scale is based upon the assumptions that one phospholipid head group occupies 0.65 nm^2 of the membrane surface and that one turn of helix occurs each 0.54 nm.

1993; Mishra et al., 1994). Second, as a constituent of factor VIII this peptide is apparently constrained by a disulfide bond linking the C-terminus and the N-terminus of the C2 domain (Figure 1). Thus, if the long axis of the membrane was perpendicular to and penetrating the membrane, then a corresponding region in the N-terminal region of the C2 domain would also be required to penetrate the membrane. Experiments with peptides from this region of the molecule (Foster et al., 1990) and antibodies recognizing the N-terminal region of the C2 domain have not suggested membrane-binding properties for this portion of the molecule.

In the model depicted in Figure 11 hydrophobic residues Ile 6, Pro 8, Trp 11, Val 12, and Ile 15 and Met 19 penetrate the hydrophobic core of the membrane and interact with phospholipid acyl chains. We speculate that π electrons of Trp 11 interact with π electrons of double bonds in adjacent acyl chains accounting for the preferential binding of factor VIII to membranes containing double bonds in phosphatidylcholine acyl chains (Gilbert & Drinkwater, 1993). The peptide backbone lies in the interfacial region of the membrane and protrudes into the aqueous region above the membrane. Both amine and carbonyl moieties of the backbone probably participate in hydrogen bonds with adjacent phospholipids. The side chain of Arg 5 extends toward the hydrophobic face and may participate in salt bridges with phosphate moieties of adjacent phospholipids. Likewise, Arg 18 extends toward the hydrophobic face of the peptide and may form salt bridges with phosphate moieties. The side groups of His 7 and His 13 are located away from the hydrophobic membrane face and may interact with surface water or form additional salt bridges with phosphatidylserine carboxyls. We note that Arg 5 and Arg 18 are conserved in the corresponding factor V sequence (Figure 1) and that, except for Val 12, the residues contributing to the hydrophobic face correspond to hydrophobic residues of factor V. Thus, the corresponding peptide from factor V may form a membrane-binding structure with essentially the same features as $fVIII_{2303-24}$. This model provides a basis for ongoing studies to determine which amino acid residues actually penetrate the micelle and to determine which amino acid residues and which corresponding properties are critical for the membrane-binding function.

Ideally, the structure of a membrane-binding peptide such as $fVIII_{2303-24}$ would be determined with the peptide bound to phospholipid vesicles. However, because phospholipid vesicles are large they tumble slowly relative to ^1H spin correlation times and the resulting broad ^1H NMR spectral lines from vesicle-bound peptides preclude high-resolution studies. We have approached this problem by studying the structure of $fVIII_{2303-24}$ in the presence of detergent micelles. The micelles, composed of amphipathic detergent monomers, are believed to provide an environment resembling the interfacial and internal regions of membranes, and because they are small, they tumble rapidly such that high-resolution NMR spectra are obtainable. Despite the tendency of SDS to denature large proteins, it preserves or induces secondary structure in membrane-binding and membrane-penetrating peptides (Tanford & Reynolds, 1976). In future studies we anticipate refining the micelle membrane model by using perdeuterated lauryl phosphorylcholine, which forms micelles with an outer surface that is chemically similar to phosphatidylcholine membranes (Macquaire et al., 1993). We will further improve the membrane simulation by adding protonated phosphatidylserine to form mixed micelles, and we will search for intermolecular NOEs between peptide and the phosphatidylserine head group. Our initial studies with the addition of protonated phosphatidylserine to deuterated SDS show chemical shift changes in the amides of Arg 5, Ile 6, His 7, Gln 9, Ser 10, Leu 17, the α proton of Arg 5, and the ϵ protons of Arg 2 and Arg 5. However, these chemical shift changes are small (<0.1 ppm), and no intermolecular NOEs were observed, possibly owing to the high concentration of competing sulfate groups from SDS.

$FVIII_{2303-24}$ resembles factor VIII in binding to phosphatidylserine on a plastic surface and binding to phosphatidylserine-containing membranes. However, the affinity of $fVIII_{2303-24}$ for sites on these membranes, with an apparent K_D of 3 μM, is about 1000 times lower than the affinity of factor VIII (Gilbert et al., 1990). This difference may be explained by the fact that the peptide must fold into the membrane-binding conformation whereas in factor VIII the binding conformation may be maintained by interaction of this peptide with other portions of the protein. Alternatively, it is possible that some of the binding energy or specificity with which factor VIII interacts with membranes arises through a second membrane-binding region as is apparently the case for the homologous protein, factor V (Kalafatis et al., 1994).

Kaiser and Kezdy (1983) noted that membrane-binding peptides have sequences that suggest they fold into amphipathic helices upon contacting a phospholipid bilayer. Indeed, peptide analogs of apolipoprotein A-1, mellitin, and β-endorphin, in which the putative helix forming residues had been entirely replaced by other helix-forming sequences, bound to phospholipid membranes much like the parent peptides and exhibited biologic activity. This suggested that no particular amino acids were critical to support the membrane-binding function, rather that the capacity to fold into an amphipathic helix determined membrane-binding function. Subsequent experiments have confirmed that amphipathic helix-forming peptides bind to membranes and that a helical peptide conformation is induced upon binding (Reynaud et al., 1993). Features that influence membrane-binding are the hydrophobic surface area (McLean et al., 1991), the net charge of the peptide and the membrane surface (Seelig & Macdonald, 1989; Beschiaschvili & Seelig, 1990; Swanson & Roise, 1992; Reynaud et al., 1993; Seelig

et al., 1993), and the location of positively charged amino acids relative to the hydrophobic surface (Mishra et al., 1994). $FVIII_{2303-24}$ resembles prior examples of membrane-binding peptides in that the structure is an amphipathic helix. It differs from prior membrane-binding structures in that the hydrophobic surface extends beyond the helix to include a residue in an extended portion (Ile 6). $FVIII_{2303-24}$ also differs from prior membrane-binding structures in that the Arg residues at either end of the hydrophobic face are directed toward the hydrophobic face rather than away from it.

In contrast to most membrane-binding proteins, factor VIII binds with high specificity to membrane sites containing phosphatidylserine (Gilbert et al., 1992). This raises the question of whether the specificity-determining amino acids lie within $fVIII_{2303-24}$. For example, do the residues that interact with *O*-phospho-L-serine (Gilbert & Drinkwater, 1993) reside within this peptide? A prior report by Foster et al. (1990) suggests that they do. We have initiated competition binding studies with modified peptides based upon $fVIII_{2303-24}$ to determine the specificity of the interaction of $fVIII_{2303-24}$ with membrane sites and the dependence upon the particular amino acid sequence. We speculate that one or both of the Arg residues that are directed toward the membrane surface are involved in specific interaction(s) with phosphatidylserine.

ACKNOWLEDGMENT

We thank Diane Drinkwater-Pransky for excellent technical assistance, Margaret Jacobs for synthesizing the peptide, and Dr. George Busch and Sue Bennett for use of the Coulter Epics Profile flow cytometer.

SUPPLEMENTARY MATERIAL AVAILABLE

Table of the restraints used for determination of the structure and a list of coordinates for the structure with the lowest energy violations (15 pages). Ordering information is given on any current masthead page.

REFERENCES

Baleja, J. D., Moult, J., & Sykes, B. D. (1990) *J. Magn. Reson. 87*, 375−384.
Barenholz, Y., Gibbes, D., Litman, B. J., Goll, J., Thompson, T. E., & Carlson, F. D. (1977) *Biochemistry 16*, 2806−2810.
Bartles, J., Galvin, N., & Frazier, W. (1982) *Biochim. Biophys. Acta 687*, 129−136.
Bax, A., & Davis, D. G. (1985) *J. Magn. Reson. 65*, 355−360.
Beschiaschvili, G., & Seelig, J. (1990) *Biochemistry 29*, 52−58.
Bevers, E., Comfurius, P., & Zwaal, R. (1983) *Biochim. Biophys. Acta 736*, 57−66.
Church, W. R., Jernigan, R. L., Toole, J., Hewick, R. M., Knopf, J., Knutson, G. J., Nesheim, M. E., Mann, K. G., & Fass, D. N. (1984) *Proc. Natl. Acad. Sci. U.S.A. 81*, 6934−6937.
Duffy, E., Parker, E., Mutucumarana, V., Johnson, A., & Lollar, P. (1992) *J. Biol. Chem. 267*, 17006−17011.
Ernst, R. R., Bodenhausen, G., & Wokaun, A. (1987) *Principles of Nuclear Magnetic Resonance in One and Two Dimensions*, Clarendon Press, Oxford.
Foster, P. A., Fulcher, C. A., Houghten, R. A., & Zimmerman, T. S. (1990) *Blood 75*, 1999−2004.
Franklin, J. C., Ellena, J. F., Jayasinghe, S., Kelsh, L. P., & Cafiso, D. S. (1994) *Biochemistry 33*, 4036−4045.
Gilbert, G. E. (1994) *The Xase Complex. Thrombosis and Hemorrhage* (Loscalzo, J., & Schafer, A. I., Eds.) pp 37−56, Blackwell Scientific Publications, Inc., Cambridge, MA.
Gilbert, G. E., & Drinkwater, D. (1993a) *Blood 82*, 60a (abstract).
Gilbert, G. E., & Drinkwater, D. (1993b) *Biochemistry 32*, 9577−9585.
Gilbert, G. E., Furie, B. C., & Furie, B. (1990) *J. Biol. Chem. 265*, 815−822.
Gilbert, G. E., Sims, P. J., Wiedmer, T., Furie, B., Furie, B. C., & Shattil, S. J. (1991) *J. Biol. Chem. 266*, 17261−17268.
Gilbert, G. E., Drinkwater, D., Barter, S., & Clouse, S. B. (1992) *J. Biol. Chem. 267*, 15861−15868.
Havel, T. F. (1991) *Prog. Biophys. Mol. Biol. 56*, 43−78.
Hyberts, S. G., Goldberg, M. S., Havel, T. F., & Wagner, G. (1992) *Protein Sci. 1*, 736−751.
Kaiser, E. T., & Kezdy, F. J. (1983) *Proc. Natl. Acad. Sci. U.S.A. 80*, 1137−1143.
Kalafatis, M., Rand, M. D., & Mann, K. G. (1994) *Biochemistry 33*, 486−493.
Kane, W. H., & Davie, E. W. (1988) *Blood 71*, 539−555.
Macquaire, F., Baleux, F., Huynh-Dinh, T., Rouge, D., Neumann, J.-M., & Sanson, A. (1993) *Biochemistry 32*, 7244−7254.
Mann, K. G., Nesheim, M. E., Church, W. R., Haley, P., & Krishnaswamy, S. (1990) *Blood 76*, 1−16.
McDonnell, P. A., & Opella, S. J. (1993) *J. Magn. Reson., Ser. B 102*, 120−125.
McLean, L. R., Hagaman, K. A., Owen, T. J., & Krstenansky, J. L. (1991) *Biochemistry 30*, 31−37.
Mishra, V. K., Palgunachari, M. N., Segrest, J. P., & Anantharamaiah, G. M. (1994) *J. Biol. Chem. 269*, 7185−7191.
Nesheim, M. E., Pittman, D. D., Wang, J. H., Slonosky, D., Giles, A. R., & Kaufman, R. J. (1988) *J. Biol. Chem. 263*, 16467−16470.
O'Neil, J. D. J., & Sykes, B. D. (1989) *Biochemistry 28*, 699−707.
Ortel, T., Devore-Carter, D., Quinn-Allen, M., & Kane, W. (1992) *J. Biol. Chem. 267*, 4189−4198.
Plesniak, L. A., Boegeman, S. C., Segelke, B. W., & Dennis, E. A. (1993) *Biochemistry 32*, 5009−5016.
Popot, J.-L. (1993) *Curr. Opin. Struct. Biol. 3*, 532−540.
Pusey, M. L., & Nelsestuen, G. L. (1984) *Biochemistry 23*, 6202−6210.
Reynaud, J. A., Grivet, J. P., Sy, D., & Trudelle, Y. (1993) *Biochemistry 32*, 4997−5008.
Sandberg, H., Bode, A., Dombrose, F., Hoechli, M., & Lentz, B. (1985) *Thromb. Res. 39*, 63−79.
Seelig, A., & Macdonald, M. (1989) *Biochemistry 28*, 2490−2496.
Seelig, J., Nebel, S., Ganz, P., & Bruns, C. (1993) *Biochemistry 32*, 9714−9721.
Shima, M., Scandella, D., Yoshioka, A., Nakai, H., Tanaka, I., Kamisue, S., Terada, S., & Fukui, H. (1993) *Thromb. Haemostasis 69*, 240−246.
Sims, P., & Wiedmer, T. (1986) *Blood 68*, 556−551.
Sims, P., Faioni, E., Wiedmer, T., & Shattil, S. (1988) *J. Biol. Chem. 263*, 18205−18212.
Stubbs, J., Lekutis, C., Singer, K., Bui, A., Yuzuki, D., Srinivasan, U., & Parry, G. (1990) *Proc. Natl. Acad. Sci. U.S.A. 87*, 8417−8421.
Swanson, S. T., & Roise, D. (1992) *Biochemistry 31*, 5746−5751.
Tanford, C., & Reynolds, J. A. (1976) *Biochim. Biophys. Acta 457*, 133−170.
Tytler, E. M., Segrest, J. P., Epand, R. M., Nie, S. Q., Epand, R. F., Mishra, V. K., Venkatachalpathi, Y. V., & Anantharamaiah, G. M. (1993) *J. Biol. Chem. 268*, 22112−22118.
van de Waart, P., Bruls, H., Hemker, H. C., & Lindhout, T. (1983) *Biochemistry 22*, 2427−2432.
Wang, Z., Jones, J. D., Rizo, J., & Gierasch, L. M. (1993) *Biochemistry 32*, 13991−13999.
Wishart, D. S., Sykes, B. D., & Richards, F. M. (1991) *J. Mol. Biol. 222*, 311−333.
Wolf, P. (1967) *Br. J. Haematol. 13*, 269.
Wüthrich, K. (1986) *NMR of Proteins and Nucleic Acids*, Wiley, New York.
Xue, J. C., Kung, C., Kalafatis, M., & Mann, K. G. (1993a) *Blood 82*, 338a (abstract).
Xue, J. C., Kalafatis, M., & Mann, K. G. (1993b). *Biochemistry 32*, 5917−5923.

BI942604J